This article was downloaded by: [Universiti Sains Malaysia]
On: 28 February 2013, At: 04:18
Publisher: Taylor & Francis
Informa Ltd Registered in England and Wales Registered Number: 1072954 Registered office: Mortimer House, 37-41 Mortimer Street, London W1T 3JH, UK

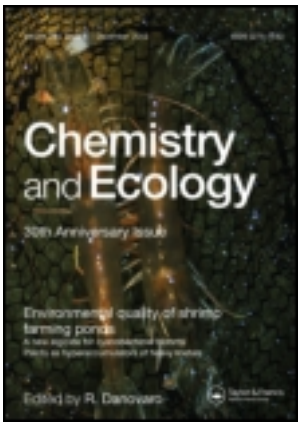

Chemistry and Ecology
Publication details, including instructions for authors and subscription information:
http://www.tandfonline.com/loi/gche20

Ackee apple (Blighia sapida) seeds: a novel adsorbent for the removal of Congo Red dye from aqueous solutions

Olugbenga S. Bello [a], Manase Auta [b] & Olumide B. Ayodele [c]

[a] Department of Pure and Applied Chemistry, Ladoke Akintola University of Technology, Ogbomoso, Nigeria

[b] Department of Chemical Engineering, Federal University of Technology, Minna, Nigeria

[c] National Engineering Design Development Institute, Nnewi, Nigeria

Version of record first published: 24 May 2012.

To cite this article: Olugbenga S. Bello , Manase Auta & Olumide B. Ayodele (2013): Ackee apple (Blighia sapida) seeds: a novel adsorbent for the removal of Congo Red dye from aqueous solutions, Chemistry and Ecology, 29:1, 58-71

To link to this article: http://dx.doi.org/10.1080/02757540.2012.686606

PLEASE SCROLL DOWN FOR ARTICLE

Full terms and conditions of use: http://www.tandfonline.com/page/terms-and-conditions

This article may be used for research, teaching, and private study purposes. Any substantial or systematic reproduction, redistribution, reselling, loan, sub-licensing, systematic supply, or distribution in any form to anyone is expressly forbidden.

The publisher does not give any warranty express or implied or make any representation that the contents will be complete or accurate or up to date. The accuracy of any instructions, formulae, and drug doses should be independently verified with primary sources. The publisher shall not be liable for any loss, actions, claims, proceedings, demand, or costs or damages whatsoever or howsoever caused arising directly or indirectly in connection with or arising out of the use of this material.

Chemistry and Ecology, 2013
Vol. 29, No. 1, 58–71, http://dx.doi.org/10.1080/02757540.2012.686606

Taylor & Francis
Taylor & Francis Group

Downloaded by [Universiti Sains Malaysia] at 04:18 28 February 2013

Ackee apple (*Blighia sapida*) seeds: a novel adsorbent for the removal of Congo Red dye from aqueous solutions

Olugbenga S. Bello[a]*, Manase Auta[b] and Olumide B. Ayodele[c]

[a]*Department of Pure and Applied Chemistry, Ladoke Akintola University of Technology, Ogbomoso, Nigeria;* [b]*Department of Chemical Engineering, Federal University of Technology, Minna, Nigeria;* [c]*National Engineering Design Development Institute, Nnewi, Nigeria.*

(*Received 6 October 2011; final version received 22 March 2012*)

The ability of ackee apple (AA) seeds to remove Congo Red (CR) dye from aqueous solution was investigated. AA was characterised using thermo gravimetric analyser, scanning electron microscopy, Braunauer Emmett Teller, pH_{pzc}, elemental analysis and Boehm titration. The effects of operational parameters such as adsorbent dosage, contact time, initial dye concentration and solution pH were studied in a batch system. pH has a profound influence on the adsorption process. Maximum dye adsorption was observed at pH 3.0. The reaction was fast, reaching equilibrium in 90 min. Adsorption data were best described by Langmuir isotherm and the pseudo-second-order kinetic model with a maximum monolayer coverage of 161.89 $mg \cdot g^{-1}$. Both boundary layer and intraparticle diffusion mechanisms were found to govern the adsorption process. Thermodynamic parameters such as standard free energy change (ΔG^0), standard enthalpy change (ΔH^0), and standard entropy change (ΔS^0) were studied. Values of ΔG^0 varied between -30.94 and -36.56 $kJ \cdot mol^{-1}$, ΔH^0 was 25.61 $kJ \cdot mol^{-1}$, and ΔS^0 was 74.84 $kJ \cdot mol^{-1} \cdot K^{-1}$, indicating that the removal of CR from aqueous solution by AA was spontaneous and endothermic in nature. Regeneration and reusability studies were carried out using different eluents. AA gave the highest adsorption efficiency up to four cycles when treated with 0.3 M HCl. AA was found to be an effective adsorbent for the removal of CR dye from aqueous solution.

Keywords: ackee apple; Congo Red; equilibrium; isotherm; spontaneous

1. Introduction

Effluents from textile, paper and pulp, paint, printing and cosmetic industries must be treated to reduce the concentration of dyes present within permissible limits before discharge into water bodies, as required by environmental regulations [1–3]. Most of these dyes are harmful when in contact with living tissues for a long time. The discharge of dyes into rivers and streams without proper treatment results in irreparable damage to crops and living organisms, both aquatic and terrestrial. Dyes are classified into three broad categories: (1) anionic – direct, acid and reactive dyes; (2) cationic – all basic dyes; and (3) nonionic – dispersed dyes [4]. Congo Red (CR) dye is an example of an anionic diazo dye and is prepared by coupling tetrazotised benzidine with two molecules of napthionic acid. It is the first synthetic dye produced that is capable of dyeing cotton directly. CR-containing effluents are generated by the textile, printing and dyeing, paper, rubber and plastics industries. As a result of its structural stability, it is difficult to biodegrade in

*Corresponding author. Email: osbello@yahoo.com

© 2013 Taylor & Francis

wastewaters. Adsorption is considered to be an attractive option in treating such wastewater [5–10], and adsorption using activated carbon is a common and popular method because of its relatively efficient dye removal. However, activated carbon has some drawbacks such as slow adsorption kinetics and low adsorption capacity of bulky adsorbate due to its microporous nature. Therefore, adsorbents should have a high surface area with large pores, as well as selective adsorption sites [11–14]. In addition, wastewater containing anionic dyes such as CR often contains other cationic and neutral pollutants, and the presence of large amounts of these pollutants in wastewater sometimes reduces the effectiveness of the adsorbents because the sorption of cationic and neutral dye pollutants depress the sorption capacity and efficiency of these adsorbents [15]. Therefore, it is very imperative to find new adsorbents with high selectivity for anionic dyes for the versatile treatment of wastewaters.

Ackee (*Blighia sapida*) is an underutilised tree crop native to West Africa and widespread in tropical and subtropical environments [16]. It is commonly known as 'Isin' among the Yoruba tribes of Nigeria, and is a wild food plant that belongs to the family Sapidaceae. The fruit is like a capsule comprising three fleshy valves that splits open when mature and ripe, displaying glossy black elongated seeds with cream-coloured arils at their base. To the best of our knowledge, no report has been documented in the literature on the adsorption of CR dye using ackee apple seeds. In this study, ackee apple seed was used as a novel nonconventional adsorbent for the removal of CR dye from aqueous solutions. Ackee apple fruit produce solid waste such as peel/skin and seeds. The amount of seed discarded is ~25–30% of its weight. Massive amounts of these seeds are disposed of, causing severe problems in the community. In an attempt to place a value on this waste and eradicate this problem, the seeds were used as an adsorbent to remove CR from aqueous solutions.

Downloaded by [Universiti Sains Malaysia] at 04:18 28 February 2013

2. Materials and methods

2.1. *Adsorbate*

CR is an anionic azo dye with the IUPAC name: 1-napthalenesulfonic acid, 3,3-(4,4-biphenylenebis(azo))bis(4-aminodisodium) salt; molecular formula, $C_{32}H_{22}N_6Na_2O_6S_2$; molecular mass, 696.68 g·mol^{-1}; CI number, 22 120; λ_{max}, 497 nm. CR was obtained from M/s Merck and a stock solution was prepared in deionised water. All other test solutions were prepared by diluting the stock solution with deionised water.

2.2. *Preparation of ackee apple seeds adsorbent*

Seeds were collected from mature and ripe fruits that had fallen from ackee apple trees in three locations within Ogbomoso metropolis (8°07′N, 4°16′E) in southwestern Nigeria. The seeds were washed with distilled water, boiled with water for 60 min, filtered and dried in an oven at 105 °C for 24 h. The dried materials were crushed and sieved to the desired mesh size (125–250 μm). The prepared ackee apple seed sample, referred to as AA, was stored in an airtight container until further use. No other chemical or physical treatments were carried out prior to the adsorption experiments.

2.3. *Batch equilibrium studies*

Batch equilibrium tests were carried out for adsorption of CR dye on AA. The effects of initial dye concentration, contact time, temperature and solution pH on dye uptake were investigated. Sample

solutions were withdrawn at equilibrium to determine residual concentrations. Solutions were filtered prior to analysis to minimise interference of the carbon fines. For equilibrium studies, the experiment was carried out for 120 min to ensure that equilibrium was reached. The linear Lambert relationship between absorbance and concentration with the calibration curve was established by plotting a graph of absorbance versus the concentration of the dye solution. The concentration of the CR dye solution before and after adsorption was determined using a double UV–Vis spectrophotometer (UV-1800 Shimadzu, Japan) at a maximum wavelength of 497 nm. The amount of CR dye adsorbed at equilibrium, q_e (mg·g^{-1}) was calculated. For the batch kinetic studies, the same procedure was followed, but the aqueous samples were taken at preset time intervals. The concentrations of CR dye were similarly measured. The CR dye uptake at any time, q_t (mg·g^{-1}), was calculated.

Downloaded by [Universiti Sains Malaysia] at 04:18 28 February 2013

2.4. *Effect of initial CR dye concentration, contact time and solution temperature*

Aliquots (100 mL) of CR dye solution with initial concentrations of 50–300 mg·L^{-1} were prepared in a series of 250-mL Erlenmeyer flasks. An equal mass of 0.20 g of AA were added to each flask, covered with glass stopper and the flasks were placed in an isothermal waterbath shaker (Model Protech, Malaysia) at 303 K and a rotation speed of 120 rpm until equilibrium was reached. The effect of solution temperature on the CR dye adsorption process was examined by varying the adsorption temperature to 303, 318 and 333 K by adjusting the temperature controller of the waterbath shaker.

2.5. *Effect of solution pH*

The effect of solution pH on the CR dye adsorption process was studied by varying the initial pH of the solution from 3 to 10. The pH was adjusted by adding 0.1 M hydrochloric acid (HCl) and/or 0.1 M sodium hydroxide (NaOH), and was measured using a pH meter (Model Delta 320, Mettler Toledo, China). The initial concentration of the CR dye was fixed at 100 mg·L^{-1} with an adsorbent dosage of 0.2 g. The solution temperature was maintained at 303 K. Percentage dye removal was calculated using Equation (1).

$$\text{Removal } (\%) = \frac{(C_0 - C_e)}{C_0} \times 100 \tag{1}$$

2.6. *Characterisation of AA*

The specific surface area and pore structure of the AA were determined by using surface area and a pore size analyser (Quantachrome, Autosorb-I) on nitrogen adsorption at 77 K. The surface morphology of the samples was examined using a scanning electron microscope (SEM; Model VPFESEM Supra 35VP). Proximate analysis was carried out using a thermogravimetric analyser (TGA; Perkin–Elmer TGA7, USA) and elemental analysis was performed using an elemental analyser (Perkin–Elmer Series 11, 2400, USA). A series of 50 mL of a 0.01 M NaCl solution was placed in a closed Erlenmeyer flask. The pH was adjusted to between 2 and 12 by adding 0.1 M HCl or 0.1 M NaOH solution. Then 0.15 g of each AA sample was added and agitated at 150 rpm for 48 h under atmospheric conditions. The final pH was measured and the results were plotted with pH (Initial pH – Final pH) against final pH. The pH_{pzc} is the point at which the curve pH_{final} versus $pH_{initial}$ crosses the line $pH_{initial} = pH_{final}$ [17].

The Boehm titration method was used to determine the number of surface functional groups. A 1 g sample of AA was weighed carefully and placed in a vial containing 25 mL of 0.1 M aqueous

solutions of: hydrochloric acid, sodium hydroxide, sodium carbonate, sodium bicarbonate and sodium ethoxide. These vials were then sealed, stirred by shaking for 48 h at 25 °C and filtered. Then, 5 mL of each filtrate was pipetted and the excess base or acid contained therein was titrated with HCl or NaOH, respectively. The numbers of different acidic sites were then calculated assuming that NaOH neutralises carboxylic, hydroxylic (phenolic) and lactonic groups, Na_2CO_3 neutralises carboxylic and lactonic groups, $NaHCO_3$ neutralises only carboxylic groups, and sodium ethoxide neutralises carbonyl groups (in aqueous solutions). The number of basic sites was calculated from the amount of HCl that reacted with the basic groups of the carbon surfaces [18].

3. Results and discussion

3.1. *Characterisation of AA adsorbent*

Elemental analysis of AA is shown in Table 1. The carbon content of AA is high. However, the hydrogen and nitrogen contents are significantly low. Similarly, proximate analysis revealed 10.42% moisture, 18.03% volatile matter, 60.14% fixed carbon and 11.41% ash content. The higher percentage of fixed carbon makes AA satisfactory for CR dye adsorption. A SEM of AA is shown in Figure 1. The SEM image shows well-developed pores at the surface. These pores allowed a good surface for CR dye to be trapped and adsorbed into [19]. The Braunauer Emmett Teller surface area, micropore volume and average pore diameter are reported in Table 2. The average pore diameter of AA was found to be 2.86 nm. This indicated that AA was mesoporous. AA has a high value for both the mesopore volume and the mesopore contribution to the porous texture (>70%). This explains the reason behind its high adsorption efficiency. This leads to the

Table 1. Proximate and elemental analyses of AA.

	Proximate analysis (%)				Elemental analysis (%)			
Sample	Moisture	Volatile	Fixed carbon	Ash	C	H	N	(S + O)[a]
AA	10.42	18.03	60.14	11.41	62.67	3.62	0.56	33.15

Note: [a]Estimated by difference.

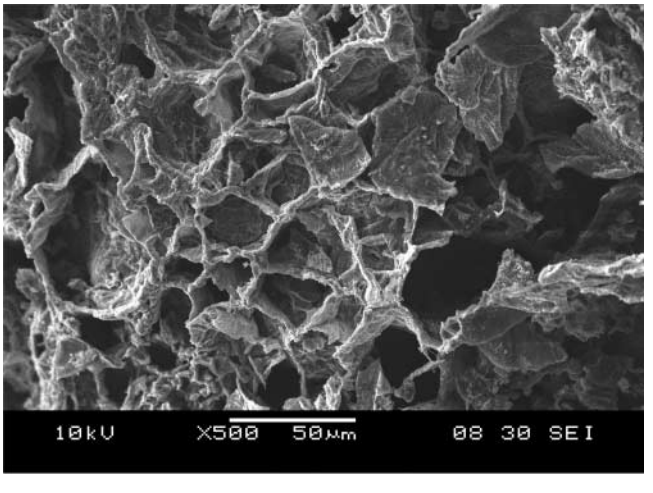

Figure 1. SEM micrograph of AA (×500).

Downloaded by [Universiti Sains Malaysia] at 04:18 28 February 2013

Table 2. Surface pore characteristics of AA.

S_{BET} ($m^2 \cdot g^{-1}$)	V_{mic} ($cm^3 \cdot g^{-1}$)	V_{mes} ($cm^3 \cdot g^{-1}$)	V_{tot} ($cm^3 \cdot g^{-1}$)	V_{mes}/V_{tot} (%)	D_p (nm)
681	0.127	0.426	0.553	77.03	2.86

Note: D_p, average pore diameter; S_{BET}, Braunauer Emmett Teller surface area; V_{mes}, mesopore volume; V_{mic}, micropore volume; V_{tot}, total volume (mic + meso).

conclusion that mesopores not only act as transporting arteries, but also contribute to the adsorption of CR dye on the adsorbent. A similar result was obtained by Gryglewicz and Lorenc-Grabowska in the adsorption of CR dye on coal based mesoporous activated carbon [20].

Downloaded by [Universiti Sains Malaysia] at 04:18 28 February 2013

3.2. *Batch equilibrium studies*

3.2.1. *Effect of pH*

The surface acidity and basicity strengths of AA obtained via the Boehm titration method are: carboxylic, $0.782\,meq \cdot g^{-1}$; lactonic, $0.541\,meq \cdot g^{-1}$; phenolic, $0.632\,meq \cdot g^{-1}$; acidic, $1.955\,meq \cdot g^{-1}$; basic, $0.618\,meq \cdot g^{-1}$; and pH_{pzc}, 4.6, respectively. These data suggest that the numbers of acidic groups on the surface of AA were greater than those of basic groups. This is in agreement with the pH_{pzc} of AA which is 4.6. Figure 2 shows that complexation of CR dye with the surface of AA was significantly affected by the solution pH. Maximum adsorption was observed at pH 3 (the extent of adsorption is ~98%). At low pH, the protonation of –OH and –COOH groups present at AA surface occurs (because pH_{pzc} for AA is 4.6, below which the adsorbent surface is positive). Newconbe and Drikas [21] reported that carboxyl groups have a pK_a value between 3.0 and 5.0. At pH values lower than pK_a, the carboxylate group carries a positive charge resulting in electrostatic attraction between the negatively charged SO_3^- groups in the dye molecule and the positively charged AA surface. Hydrogen bonding between oxygen and nitrogen containing functional groups of CR dye and the AA surface is another factor contributing to the higher adsorption at low pH. However, at high pH, the carboxylic groups of AA are expected to ionise completely. Therefore, electrostatic repulsion between anionic CR dye and the negatively charged surface of AA lowers the adsorption capacity, resulting in the low adsorption capacity observed at pH 11 (the extent of the adsorption is 38%). Similar results were obtained by Binupriya et al. [22], Chowdhury et al. [23] and Ahmad and Kumar [24].

3.2.2. *Effect of initial dye concentration and temperature on adsorption*

Five different concentrations, 50, 100, 150, 200 and $300\,mg \cdot L^{-1}$, were selected to investigate the effect of CR dye concentration (C_0) on AA. The result obtained at 303 K at the pH (3.02) of the CR dye solution is shown in Figure 3. As shown in Figure 3, with increasing initial dye concentrations from 50 to $300\,mg \cdot L^{-1}$, the amount of dye adsorbed by AA increases from 38.98 to $214.67\,mg \cdot g^{-1}$. Figure 3 also shows that the adsorption of CR dye is fast at the initial stage, and then becomes slower near equilibrium. This is a result of the large number of vacant surface sites that are available for adsorption during the initial stages, after some time, the remaining vacant surface sites are difficult to occupy because of repulsive forces between the CR dye adsorbed on the surface of AA and the solution phase. It is evident that the adsorption process is highly dependent on the initial concentration of the solution. The increase in the equilibrium adsorption of CR dye on AA with temperature revealed that higher temperatures favour CR dye removal via adsorption onto AA. This is due to the increasing mobility of the large dye ion with a rise in temperature [25,26].

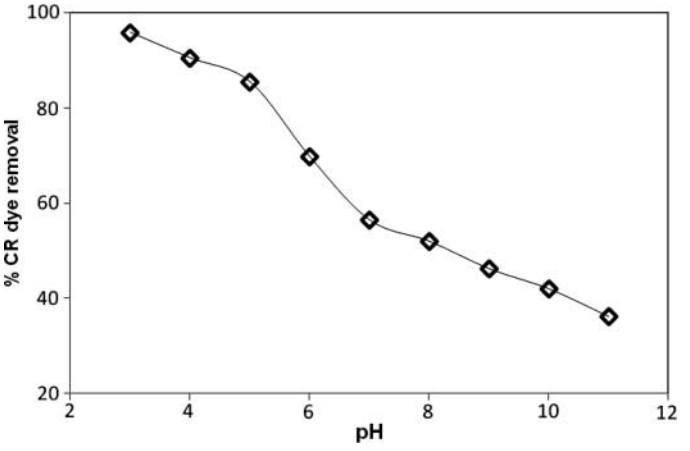

Figure 2. Effect of pH on the adsorption of CR dye by AA (Conditions: 0.2 g adsorbent dosage, 120 rpm, temperature 303 K).

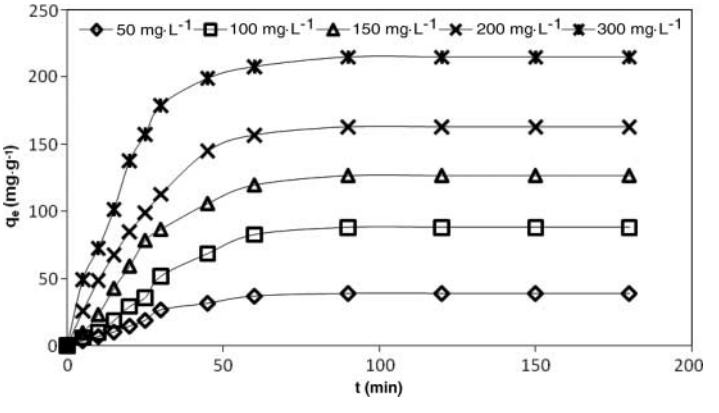

Figure 3. Effect of initial dye concentration on the adsorption of CR dye by AA (Conditions: 0.2 g adsorbent dosage, 120 rpm, 120 min agitation time, temperature 303 K).

3.2.3. *Effect of contact time and adsorbent dosage*

The effect of contact time on CR dye adsorption onto AA at different concentrations is shown in Figure 4. The particle size of AA used is 200 μm. CR dye adsorption increases as the initial concentration increases. Figure 4 shows that the adsorption of CR dye was in two phases: (2) an initial rapid phase in which adsorption capacity increased sharply within the first 60 min due to rapid surface adsorption (external surface adsorption); and (2) a slower phase whose contribution to the total amount of dye adsorption was relatively small (internal surface adsorption) [27]. Adsorption equilibrium was achieved within 90 min, after which the amount of dye adsorption becomes negligible. The initial sorption rate, h was highest at 0.2 g dosage, 40.13 $mg \cdot g^{-1} \cdot min^{-1}$ (Figure 4). 0.2 g was used as adsorbent dosage throughout the adsorption experiment.

3.3. *Kinetics of adsorption*

The adsorption data were tested using three well-known models: pseudo-first-order, pseudo-second-order and the intraparticle diffusion models. The pseudo-first-order kinetic model of

Downloaded by [Universiti Sains Malaysia] at 04:18 28 February 2013

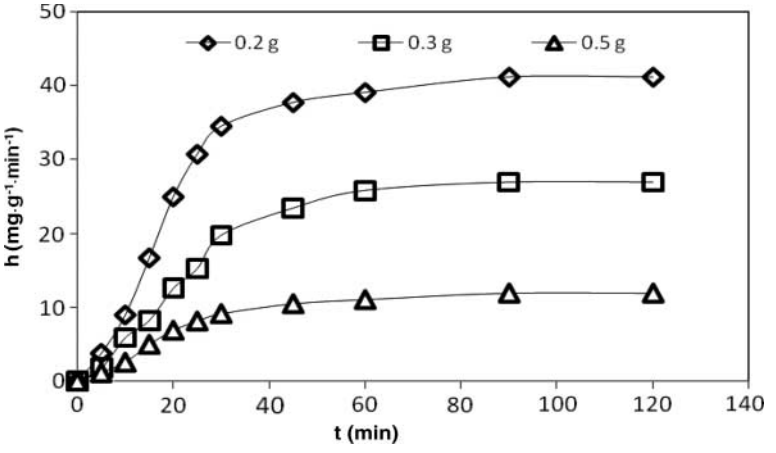

Figure 4. Effect of adsorbent dosage on the adsorption of CR dye by AA (Conditions: pH 3, 120 rpm, 120 min agitation time, temperature 303 K).

Lagergren [28] is given by:

$$\ln(q_e - q_t) = \ln q_e - k_1 t \tag{2}$$

where q_e and q_t are the adsorption capacities at equilibrium and at time t respectively (mg·g^{-1}), and k_1 is the rate constant for pseudo-first-order adsorption (min^{-1}). A plot of ln $(q_e - q_t)$ against t at various concentrations and temperatures resulted in linear graphs with negative slopes (figure not shown). k_1 and q_e are calculated from the slopes and intercepts, respectively. Although, the correlation coefficients (R^2) were high, but comparison of $q_{e\,\text{calc.}}$ with $q_{e\,\text{exp.}}$ values do not agree (Table 3). Therefore, the adsorption of CR dye onto AA does not follow pseudo-first-order kinetics. The pseudo-second-order rate equation can be expressed in the following form [29]:

$$\frac{t}{q_t} = \frac{1}{k_2 q_e^2} + \frac{1}{q_e} t \tag{3}$$

If the initial adsorption rate, h (mg·g^{-1}·min^{-1}) is

$$h = k_2 q_e^2 \tag{4}$$

Plots of t/q_t versus t gave linear graphs from which q_e and k_2 were estimated from the slopes and intercepts of the plot (not shown) for temperatures ranging from 303–333 K. The R^2 values were as high as 0.99 and there was good agreement between $q_{e,\text{cal.}}$ and $q_{e,\text{exp}}$ obtained (Table 3). The good agreement shows that the pseudo-second-order kinetic equation fits the adsorption data well. The intraparticle diffusion equation [30] is given by:

$$q_t = k_{ip} t^{1/2} + C \tag{5}$$

where q_t is the amount of dye adsorbed (mg·g^{-1}) at time t, and k_{ip} (mg·g^{-1}·min$^{1/2}$) is the rate constant for intraparticle diffusion. The values of q_t correlated linearly with values of $t^{1/2}$ (Figure 5) and the rate constant k_{ip} directly evaluated from the slope of regression line. The value of C gives an idea of the thickness of boundary layer, the larger the intercept, the greater the boundary layer effect. From the plots of q_t against $t^{1/2}$ at various initial CR dye concentrations, multilinear profiles were observed (Figure 5) indicating that intraparticle diffusion plays a significant role, but is not the only rate-controlling step. The first and sharper portion is attributed to the boundary layer diffusion of CR dye molecules, whereas the second portion corresponds to the gradual adsorption

Downloaded by [Universiti Sains Malaysia] at 04:18 28 February 2013

Downloaded by [Universiti Sains Malaysia] at 04:18 28 February 2013

Table 3. Parameters of different kinetic models of CR dye adsorption onto AA.

		Pseudo-first-order model			Pseudo-second-order model				Intraparticle diffusion model					
Adsorption condition	$q_{e,\exp}$ ($mg \cdot g^{-1}$)	k_1 (min^{-1})	$q_{e,cal}$ ($mg \cdot g^{-1}$)	R^2	$k_2 \times 10^{-3}$ ($g \cdot mg^{-1} \cdot min^{-1}$)	$q_{e,cal}$ ($mg \cdot g^{-1}$)	R^2	h	k_{i1} ($mg \cdot g^{-1} \cdot min^{1/2}$)	C	R^2	k_{i2} ($mg \cdot g^{-1} \cdot min^{1/2}$)	C	R^2
Concentration ($mg \cdot L^{-1}$)														
50	38.98	0.076	30.41	0.95	0.396	40.14	0.99	0.64	6.76	53.76	0.88	1.64	108.67	0.92
100	87.98	0.094	75.89	0.91	0.478	88.91	0.99	3.78	8.91	60.13	0.86	1.78	92.54	0.91
150	126.43	0.116	107.15	0.96	0.521	127.41	0.99	8.46	10.84	71.67	0.94	1.87	88.14	0.94
200	162.87	0.149	141.98	0.93	0.567	164.13	0.99	15.04	12.13	82.45	0.92	1.94	82.18	0.93
300	214.67	0.196	197.82	0.94	0.612	216.45	0.99	28.20	14.22	95.17	0.95	2.01	76.45	0.94
Temp (K)														
303	160.75	0.049	152.96	0.89	0.423	163.51	0.99	10.93	8.16	55.24	0.85	1.75	67.56	0.93
318	183.32	0.067	179.17	0.96	0.526	188.13	0.99	17.68	10.94	48.91	0.93	2.06	59.45	0.92
333	201.78	0.086	188.89	0.93	0.601	199.58	0.99	24.47	13.68	37.23	0.89	2.61	49.18	0.93
pH														
3	126.13	0.085	117.32	0.87	0.474	127.36	0.99	2.89	17.86	45.17	0.95	1.95	58.17	0.94
6	92.61	0.071	53.91	0.94	0.356	93.45	0.99	1.83	15.88	42.78	0.94	1.88	51.86	0.93
9	68.98	0.059	59.78	0.94	0.209	69.11	0.99	1.70	13.89	37.46	0.96	1.67	47.61	0.94
11	55.76	0.045	48.13	0.88	0.178	57.24	0.99	1.55	12.42	32.71	0.97	1.43	38.28	0.95

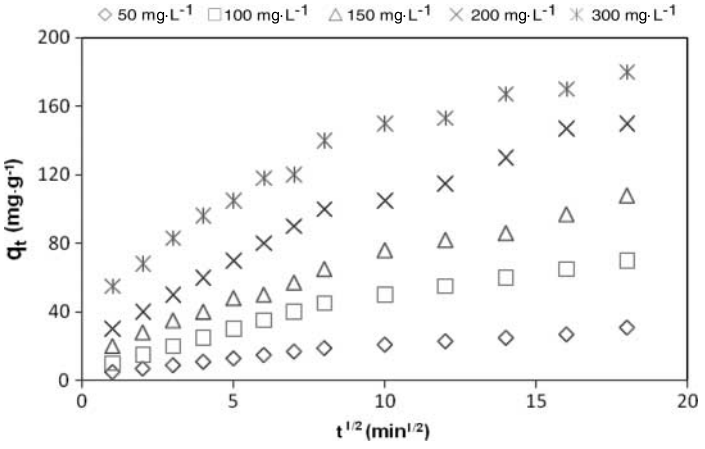

Figure 5. Intraparticle diffusion plots for the adsorption of CR dye onto AA at different dye concentrations (Conditions: 0.2 g adsorbent dosage, 120 rpm, temperature 303 K).

Downloaded by [Universiti Sains Malaysia] at 04:18 28 February 2013

stage, where intraparticle diffusion was the rate-limiting step. The slope of the second linear portion of the plot was defined as the intraparticle diffusion parameter k_{i2}. The corresponding model fitting parameters under different conditions are reported in Table 3. The observed values of k_{i2} are lower than k_{i1}, indicating that intraparticle diffusion mainly controls the adsorption rate. However, external mass transfer resistance cannot be neglected, although this is only significant during the initial period.

3.4. *Adsorption isotherm*

Adsorption isotherms are important for the description of how molecules of adsorbate interact with the adsorbent surface. Hence, two important isotherms were selected in this study: Langmuir and Freundlich. The linearised form of Langmuir adsorption model is expressed as [31]:

$$\frac{C_e}{q_e} = \frac{C_e}{q_o} + \frac{1}{q_o K_L} \tag{6}$$

where C_e is the dye concentration in the solution at equilibrium (mg·L^{-1}), q_e is the dye concentration on the adsorbent at equilibrium (mg·g^{-1}), q_o is the monolayer adsorption capacity of adsorbent (mg·g^{-1}) and K_L is the Langmuir adsorption constant (L·mg^{-1}). A nonlinear plot of C_e against q_e is shown in Figure 6. The R^2 values for the Langmuir isotherm, when compared with the Freundlich isotherm, indicate that the adsorption of CR dye onto AA fits the Langmuir isotherm well. Values of q_o and b are calculated from linear plots (not shown) and reported in Table 4. Table 4 shows that AA is a promising adsorbent for CR dye. The value of q_o obtained was compared with values for other adsorbents (Table 5). The essential characteristics of the Langmuir isotherm can be expressed by a dimensionless constant called equilibrium parameter R_{L} that is defined by Equation (7):

$$R_L = \frac{1}{(1 + K_L C_o)} \tag{7}$$

where K_L and C_0 are the Langmuir adsorption constant (L·mg^{-1}) and the highest initial dye concentration (mg·L^{-1}), respectively. Values of R_{L} were calculated using Equation (7). The nature of the adsorption process could be unfavourable ($R_{\mathrm{L}} > 1$), linear ($R_{\mathrm{L}} = 1$), favourable ($0 < R_{\mathrm{L}} < 1$) or irreversible ($R_{\mathrm{L}} = 0$). The R_{L} values obtained here are listed in Table 4. The fact that all the

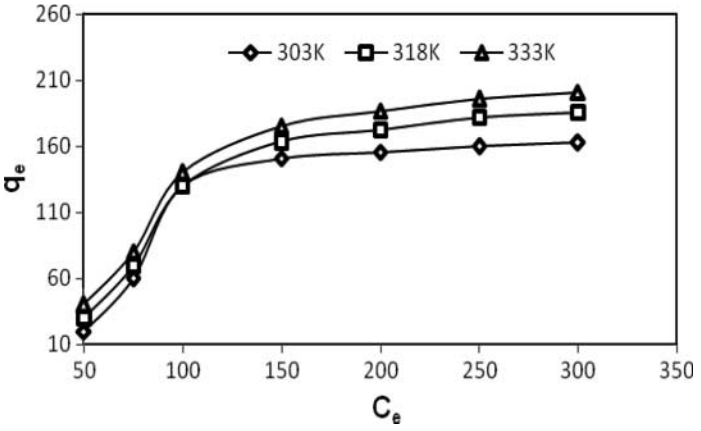

Figure 6. Langmuir adsorption isotherms for the adsorption of CR dye onto AA at different temperatures.

Table 4. Langmuir and Freundlich isotherm model statistical parameters for the adsorption of CR dye adsorption onto AA at different temperatures.

	T (K)		
Model	303	318	333
Langmuir isotherm			
q_{max} (mg·g^{-1})	161.89	186.81	198.32
K_L (L·mg^{-1})	0.31	0.52	0.78
R_L	0.43	0.54	0.66
R^2	0.99	0.99	0.99
Freundlich isotherm			
k_F	127.6	136.5	147.2
n	2.16	3.34	4.72
R^2	0.91	0.95	0.94
D–R isotherm			
q_o (mg·g^{-1})	64.38	82.46	91.67
β (mol^2·kJ^{-2})	0.052	0.041	0.036
R^2	0.94	0.97	0.95
E_a (kJ·mol^{-1})	3.10	3.49	3.73

R_L values for the adsorption of CR onto AA are in the range 0.43–0.66 shows that the adsorption process is favourable.

The linearised form of the Freundlich model is represented by:

$$\log q_e = \frac{1}{n} \log C_e + \log k_f \tag{8}$$

where q_e is the amount of CR dye adsorbed at equilibrium (mg·g^{-1}), C_e is the equilibrium concentration of the adsorbate (mg·L^{-1}); k_f and n are constants incorporating the factors affecting the adsorption capacity and the degree of nonlinearity between the solute concentration in the solution and the amount adsorbed at equilibrium [32]. Plots of log q_e versus log C_e gave linear graphs (not shown) with high R^2 values. Comparing the R^2 values with those obtained from Langmuir isotherms, the adsorption data do not fits the Freundlich isotherm well (Table 4). Values of k_f and n obtained from the slopes and intercepts of the graph reported in Table 4 shows the heterogeneity of the material, as well the possibility of multilayer adsorption of CR dye through the percolation process; values of $n > 1$ indicate that the adsorption is favourable.

Downloaded by [Universiti Sains Malaysia] at 04:18 28 February 2013

Table 5. Comparison of the maximum monolayer adsorption capacities of CR dye onto various adsorbents.

Adsorbent	q_o (mg·g^{-1})	Ref
Coir pith	6.70	[5]
Aspergilius niger biomass	8.19	[38]
Neem leaf powder	41.20	[2]
Bagasse fly ash	11.89	[9]
Activated carbon (laboratory grade)	1.88	[9]
Acid activated red mud	7.08	[39]
Mesoporous activated carbon	189	[20]
Montmorillonite	12.7	[40]
Chitosan beads	93.71	[41]
Chitosan/montmorillonite nanocomposite	54.52	[40]
4-Vinyl pyridine grafted poly(ethylene) terepthalate fibres	18.1	[42]
Aniline propysilica xerogel	22.62	[8]
Ca-bentonite	107.41	[42]
Ackee apple	161.89	This study

The D–R model [33] was also used to test the experimental data. It is expressed as:

$$\ln q_e = \ln q_o - \beta\varepsilon^2 \tag{9}$$

where β is the free energy of sorption per mole of the sorbate as it migrates to the surface of AA from an infinite distance in the solution (mol^2·kJ^{-2}), q_o is the maximum adsorption capacity and ε is the Polanyi potential (J·mol^{-1}), which can be written as

$$\varepsilon = RT \ln\left(1 + \frac{1}{C_e}\right) \tag{10}$$

where R and T are the gas constant (kJ·mol^{-1}·K^{-1}) and the absolute temperature (K), respectively. Plots of $\ln q_e$ versus ε^2 gave linear graphs (not shown) where β and q_o are obtained from the slopes and intercepts respectively (Table 4). Similarly, the β value obtained was then used to estimate the mean free energy of adsorption, E_a using the relation:

$$E_a = \sqrt{\frac{1}{2\beta}} \tag{11}$$

From Table 4, the value of E_a lies in the range 3.10–3.73 kJ·mol^{-1}. The mean energy of adsorption is the free energy change when one mole of the dye ions is transferred from infinity in the solution to the surface of the adsorbent. The value of this parameter gives information about the adsorption mechanism. When one mole of ions is transferred, its value in the range of 1–8 kJ·mol^{-1} indicates a physical adsorption mechanism [34], if the value of E_a is between 8 and 16 kJ·mol^{-1}, this indicates that the adsorption process is an ion-exchange mechanism [35], whereas a value in the range of 20–40 kJ·mol^{-1} is indicative of a chemical adsorption mechanism [36]. The results obtained showed that a physical mechanism dominates in the adsorption process.

3.5. *Adsorption thermodynamics*

To better understand the effect of temperature on the adsorption, thermodynamic parameters such as standard Gibbs free energy change, ΔG^0, standard enthalpy ΔH^0 and standard entropy ΔS^0 were studied. The Gibbs free energy of adsorption using the Langmuir constant K_L is

Downloaded by [Universiti Sains Malaysia] at 04:18 28 February 2013

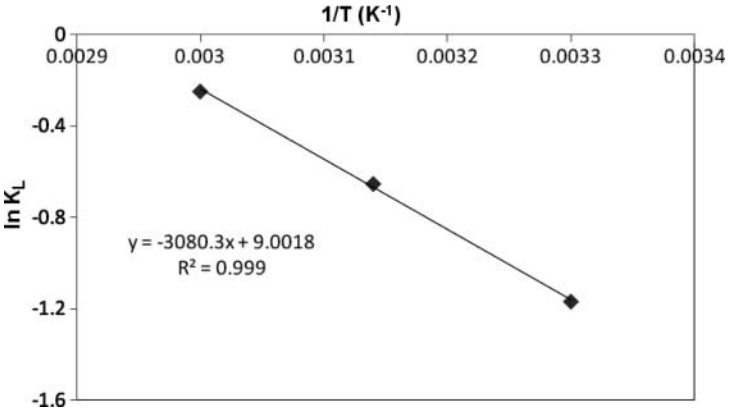

Figure 7. Van't Hoff plot of CR dye adsorption onto AA.

Table 6. Thermodynamic parameters for the adsorption of CR dye adsorption onto AA at different temperatures.

Temp (K)	$K_L \times 10^5$ (L·mol^{-1})	ΔG^0 (kJ·mol^{-1})	ΔH^0_{ads} (kJ·mol^{-1})	ΔS^0 (kJ·mol^{-1}·K^{-1})
303	2.16	−30.94	25.61	74.84
318	3.62	−33.84		
333	5.43	−36.56		

calculated from:

$$\Delta G^0 = -RT \ln K_L \tag{12}$$

Standard enthalpy ΔH^0 and standard entropy ΔS^0 can be estimated from the Van't Hoff equation:

$$\ln K_L = \frac{\Delta S^0}{R} - \frac{\Delta H^0_{ads}}{RT} \tag{13}$$

where R is the gas constant and K_L is the Langmuir adsorption constant. The plot of ln K_L against $1/T$ (in Kelvin) was linear. The slope of the Van't Hoff plot is equal to $\Delta H^0_{ads}/R$, and its intercept is equal to $\Delta S^0/R$. The Van't Hoff plot for the adsorption of CR dye onto AA is given in Figure 7. The thermodynamic parameters obtained are given in Table 6. As shown in Table 6, the negative values of ΔG^0 at different temperatures indicate the spontaneous nature of the adsorption. Values of ΔH^0_{ads} and ΔS^0 were positive, showing that the adsorption process is endothermic and there was increased randomness between the adsorbent/adsorbate interfaces during the adsorption of CR dye onto AA.

3.6. *Regeneration and reusability*

Regeneration requires proper selection of eluent, which strongly depends on the type of adsorbent and the mechanism of adsorption [37]. The selected eluent must be effective, harmless to the adsorbent, nonpolluting and cheap. For this purpose, HCl, deionised water and NaOH were used as eluents. The CR-laden adsorbent was subjected to adsorption–desorption cycles. This was achieved using 250 mL of each eluent to desorp the adsorbed dye after each round of adsorption. This regeneration step was repeated after each adsorption cycle. Table 7 shows that the efficiency of the adsorption of CR dye onto AA after treatment with different eluents. The eluent that gave the best regeneration efficiency, as evidenced by the percentage of CR dye adsorbed, was treatment with 0.3 M HCl.

Downloaded by [Universiti Sains Malaysia] at 04:18 28 February 2013

Table 7. Percentage adsorption of CR dye on regenerated AA.

Eluents used for regeneration	Dye	Adsorbent	Percentage CR dye adsorbed			
			I Cycle	II Cycle	III Cycle	IV Cycle
0.3 M HCl	CR	AA	88.97	91.76	93.18	96.84
Deionised water			61.54	63.78	67.19	69.43
0.3 M NaOH			47.82	50.15	51.43	52.21

4. Conclusions

SEM, proximate and elemental analyses revealed the adsorptive features of this novel adsorbent. The Langmuir isotherm was found to correlate most with the adsorption data, with a maximum monolayer coverage of 161.89 $mg \cdot g^{-1}$. Kinetic studies showed that the adsorption profile followed a pseudo-second-order model with a multistep diffusion process. Acidic pH was found to enhance the CR dye removal most. The regeneration and reusability of AA were assessed for four successive adsorption–desorption cycles and the adsorptive capacity was found to remain as high as 96.84% when treated with 0.3 M HCl. This study revealed that ackee apple seeds can be used as alternative adsorbents for the removal of recalcitrant CR dye from aqueous solutions.

Downloaded by [Universiti Sains Malaysia] at 04:18 28 February 2013

Acknowledgements

The one year post doctoral fellowship jointly awarded by USM-TWAS to Dr Olugbenga Solomon BELLO (FR Number: 3240223483 in Year 2009) of the Department of Pure and Applied Chemistry, Ladoke Akintola University of Technology, P.M.B 4000, Ogbomoso, Oyo State. Nigeria and the 12- month study leave granted him by his home institution to honor this fellowship are both acknowledged.

References

[1] Z. Aksu, *Application of biosorption for the removal of organic pollutants: A review*, Process Biochem. 40 (2005), pp. 997–1026.
[2] K.G. Bhattacharyya and A. Sharma, Azadirachta indica *leaf powder as an effective biosorbent for dyes: A case study with aqueous Congo red solutions*, J. Environ. Manage. 71 (2004), pp. 217–229.
[3] C. Namasivayam, R. Radhika, and S. Suba, *Uptake of dyes by a promising locally available agricultural solidwaste: Coir pith*, Waste Manage. 21 (2001), pp. 381–387.
[4] G. Mishra and M. Tripathy, *A critical review of the treatment for decolorization of textile effluent*, Colourage 40 (1993), pp. 35–38.
[5] C. Namasivayam and D. Kavitha, *Removal of Congo red from water by adsorption onto activated carbon prepared from coir pith, an agricultural solid waste*, Dye Pigments 54 (2002), pp. 47–58.
[6] V. Vimonses, S. Lei, B. Jin, C.W.K. Chow, and C. Saint, *Kinetic study and equilibrium isotherm analysis of Congo red adsorption by clay materials*, Chem. Eng. J. 148 (2009), pp. 354–364.
[7] M.K. Purkait, A. Maiti, S. DasGupta, and S. De, *Removal of Congo red using activated carbon and its regeneration*, J. Hazard. Mater. 145 (2007), pp. 287–295.
[8] F. Pavan, S. Dias, E. Lima, and E. Benvenutti, *Removal of Congo red from aqueous solution by anilinepropylsilica xerogel*, Dyes Pigments 76 (2008), pp. 64–69.
[9] I.D. Mall, V.C. Srivastava, N.K. Agarwal, and I.M. Mishra, *Removal of congo red from aqueous solution by bagasse fly ash and activated carbon: Kinetic study and equilibrium isotherm analyses*, Chemosphere 61 (2005), pp. 492–501.
[10] H. Chen and J. Zhao, *Adsorption study for removal of Congo red anionic dye using organo-attapulgite*, Adsorption 15 (2009), pp. 381–389.
[11] K. Nakagawa, A. Namba, S.R. Mukai, H. Tamon, P. Ariyadejwanich, and W. Tanthapanichakoon, *Adsorption of phenol and reactive dye from aqueous solution on activated carbons derived from solid wastes*, Water Res. 38 (2004), pp. 1791–1798.
[12] W. Tanthapanichakoon, P. Ariyadejwanich, P. Japthong, K. Nakarawa, S.R. Mukai, and H. Tamon, *Adsorption–desorption characteristics of phenol and reactive dyes from aqueous solution on mesoporous activated carbon prepared from waste tires*, Water Res. 39 (2005), pp. 1347–1353.
[13] M. Valix, W.H. Cheung, and G. McKay, *Preparation of activated carbon using low temperature carbonization and physical activation of high ash raw bagasse for acid dye adsorption*, Chemosphere 56 (2004), pp. 493–501.

[14] J.B. Joo, J. Park, and J. Yi, *Preparation of polyelectrolyte-functionalized mesoporous silicas for the selective adsorption of anionic dye in an aqueous solution*, J. Hazard. Mater. 168 (2009), pp. 102–107.
[15] S. Kagaya, H. Miyazaki, M. Ito, K. Tohda, and T. Kanbara, *Selective removal of mercury(II) from wastewater using polythioamides*, J. Hazard. Mater. 175 (2010), pp. 1113–1115.
[16] L.A. Assi, *Diversity of under-utilized species in Africa*, in *Crop Genetic Resources of Africa*, F. Attere, H. Zedan, N.Q. Ng, and P. Perrino, eds., Vol. I, International Board for Plant Genetic Resources (IBPGR)/United Nations Environment Programme (UNEP)/ International Institute of Tropical Agriculture (IITA)/Consiglio Nazionale delle Ricerche (CNR), Nairobi, 1988, pp. 53–88.
[17] P. Nowicki, H. Wachowska, and R. Pietrzak, *Active carbons prepared by chemical activation of plum stones and their application in removal of NO_2*, J. Hazard. Mater. 181 (2010), pp. 1088–1094.
[18] H.P. Boehm, *Surface oxides on carbon and their analysis: A critical assessment*, Carbon 40 (2002), pp. 145–149.
[19] N.K. Amin, *Removal of acid blue-106 dye from aqueous solution using new activated carbons developed from pomegranate peel: Adsorption equilibrium and kinetics*, J. Hazard. Mater. 165 (2008), pp. 52–62.
[20] E. Lorenc-Grabowska and G. Gryglewicz, *Adsorption characteristics of Congo red on coal-based mesoporous activated carbon*, Dyes Pigments 74 (2007), pp. 34–40.
[21] G. Newcombe and M. Drikas, *Adsorption of NOM activated carbon: Electrostatic and NON-electrostatic effects*, Carbon 35 (1997), pp. 1239–1250.
[22] A.R. Binupriya, M. Sathishkumar, D. Kavitha, K. Swaminathan, S.E. Yun, and S.P. Mun, *Experimental and isothermal studies on sorption of Congo red by modified mycelial biomass of woodrotting fungus*, Clean 35 (2007), pp. 143–150.
[23] A.K. Chowdhury, A.D. Sarkar, and A. Bandyopadhyay, *Rice husk ash as a low cost adsorbent for the removal of methylene blue and Congo red in aqueous phases*, Clean 37 (2009), pp. 581–591.
[24] R. Ahmad and R. Kumar, *Conducting polyaniline/iron oxide composite: A novel adsorbent for the removal of amido black 10B*, J. Chem. Eng. Data 55 (2010), pp 3489–3493.
[25] B.H. Hameed, A.A. Ahmad, and N. Aziz, *Isotherms, kinetics and thermodynamics of acid dye adsorption on activated palm ash*, Chem. Eng. J. 133 (2007), pp. 195–203.
[26] M. Alkan and M. Dogan, *Adsorption kinetics of Victoria blue onto perlite*, Fres. Environ. Bull. 12 (2003), pp. 418–425.
[27] A. Rais and K. Rajeev, *Adsorptive removal of Congo red dye from aqueous solution using bael shell carbon*, Appl. Surf. Sci. 257 (2010), pp. 1628–1633
[28] S. Lagergren and B.K. Svenska, *On the theory of so-called adsorption of materials*, R. Swed. Acad. Sci. Doc, Band 24 (1898), pp. 1–13.
[29] G. McKay and Y.S. Ho, *Pseudo-second order model for sorption processes*, Process Biochem. 34 (1999), pp. 451–465.
[30] W.J. Weber and J.C. Morris, *Kinetics of adsorption on carbon from solution*, J. Sanitary Eng. Div. Am. Soc. Civ. Eng. 89 (1963), pp. 31–60.
[31] I. Langmuir, *The constitutional and fundamental properties of solids and liquids*, J. Am. Chem. Soc. 38 (1916), pp. 2221–2295.
[32] H.M.F. Freundlich, *Over the adsorption in solution*, Z. Phys. Chem. 57 (1906), pp. 385–470.
[33] M.M. Dubinin and L.V. Radushkevich, *Equation of the characteristic curve of activated carbon*, Proc. Acad. Sci. Phys. Chem. USSR 55 (1947), pp. 331–333.
[34] M.S. Onyango, Y. Kojima, O. Aoyi, E.C. Bernardo, and H. Matsuda, *Adsorption equilibrium modeling and solution chemistry dependence of fluoride removal from water by trivalent-cation-exchanged zeolite F-9*, J. Colloid Interf. Sci. 279 (2004), pp. 341–350.
[35] F. Helfferich, *Ion Exchange*, McGraw-Hill, New York, 1962.
[36] S.S. Tahir and N. Rauf. *Removal of cationic dye from aqueous solutions by adsorption onto bentonite clay*, Chemosphere 63 (2006), pp. 1842–1848.
[37] K. Vijayaraghavan and Y.S. Yun, *Bacterial biosorbents and biosorption*, Biotechnol. Adv. 26 (2008), pp. 266–291.
[38] Y.Z. Fu and T. Viraraghavan, *Removal of Congo red from an aqueous solution by fungus* Aspergillus niger, Adv. Environ. Res. 7, (2002), pp. 239–247.
[39] A. Tor and Y. Cengeloglu, *Removal of Congo red from aqueous solution by adsorption onto acid activated red mud*, J. Hazard. Mater. 138 (2006), pp. 409–415.
[40] L. Wang and A. Wang, *Adsorption characteristics of Congo red onto the chitosan/ montmorillonite nanocomposite*, J. Hazard. Mater. 147 (2007), pp. 979–985.
[41] S. Chatterjee, T. Chatterjee, and S.H. Woo, *A new type of chitosan hydrogel sorbent generated by anionic surfactant gelation*, Bioresour. Technol. 101 (2010), pp. 3853–3858.
[42] M. Arslan, *Use of 1,6-diaminohexane-functionalized glycidyl methacrylateg- poly (ethylene terephthalate) fiber for removal of acidic dye from aqueous solution*, Fiber Polymer 11, (2010), pp. 177–184.
[43] L. Lian, L. Guo, and C. Guo, *Adsorption of Congo red from aqueous solutions onto Ca-bentonite*, J. Hazard. Mater. 161 (2009), pp. 126–131.

Downloaded by [Universiti Sains Malaysia] at 04:18 28 February 2013